Control of coherence transfer via tunneling in quadruple and multiple quantum dots

2016 Laser Phys. Lett. 13 125205

(http://iopscience.iop.org/1612-202X/13/12/125205)

IOP Publishing | Astro Ltd
Laser Physics Letters
Laser Phys. Lett. **13** (2016) 125205 (10pp)
doi:10.1088/1612-2011/13/12/125205

Letter

Control of coherence transfer via tunneling in quadruple and multiple quantum dots

Si-Cong Tian[1], En-Bo Xing[1,2], Ren-Gang Wan[3], Chun-Liang Wang[4], Li-Jie Wang[1], Shi-Li Shu[1], Cun-Zhu Tong[1] and Li-Jun Wang[1]

[1] State Key laboratory of Luminescence and Applications, Changchun Institute of Optics, Fine Mechanics and Physics, Chinese Academy of Sciences, Changchun 130033, People's Republic of China
[2] The University of Chinese Academy of Sciences, 100049 Beijing, People's Republic of China
[3] School of Physics and Information Technology, Shaanxi Normal University, Xi'an 710062, People's Republic of China
[4] Centre for Advanced Optoelectronic Functional Materials Research and Key Laboratory for UV Light-Emitting Materials and Technology of the Ministry of Education, Northeast Normal University, Changchun 130024, People's Republic of China

E-mail: shushili@ciomp.ac.cn and tongcz@ciomp.ac.cn

Received 25 April 2016, revised 1 October 2016
Accepted for publication 2 October 2016
Published 8 November 2016

Abstract

Transfer and manipulation of coherence among the ground state and indirect exciton states via tunneling in quadruple and multiple quantum dots is analyzed. By applying suitable amplitudes and sequences of the pump and tunneling pulses, a complete transfer of coherence or an arbitrary distribution of coherence of multiple states can be realized. The method, which is an adiabatic passage process, is different from previous works on quantum dot molecules in the way that the population can transfer from the ground state to the indirect exciton states without populating the direct exciton state, and thus no spontaneous emission occurs. This investigation can provide further insight to help the experimental development of coherence transfer in semiconductor structures, and may have potential applications in quantum information processing.

Keywords: coherence transfer, quantum dot molecules, stimulated Raman adiabatic passage

(Some figures may appear in colour only in the online journal)

1. Introduction

Quantum coherence in atoms or semiconductor structures with discrete energy levels lies at the heart of many interesting phenomena. Atomic coherence resulting from laser fields and atoms is responsible for many important physical effects, such as coherent population trapping [1–3], electromagnetically induced transparency [4–6], stimulated Raman adiabatic passage (STIRAP) [7–10] and Stark-chirped rapid adiabatic passage [11, 12]. On the other hand, atomic coherence can be created by the incoherent processes of atoms such as spontaneous emission: this type of atomic coherence is called spontaneously generated coherence [13–17].

Although atoms are excellent media for fundamental investigations of quantum coherence, they are rather unsuited to practical applications because of the complicated experimental setup [18]. The current trend is to study similar effects in solid-state systems, such as semiconductor quantum dots (QDs). One advantage of QDs is that their energy scales and physical features can be flexibly designed, not only by the composition, but also by the externally applied voltages. The creation of quantum coherence in QDs via laser fields has been demonstrated by several groups [19–22]. The process, which is known as Rabi oscillation, is a proof of the exciton qubit rotation. Furthermore, two or more QDs coupled together can form quantum dot

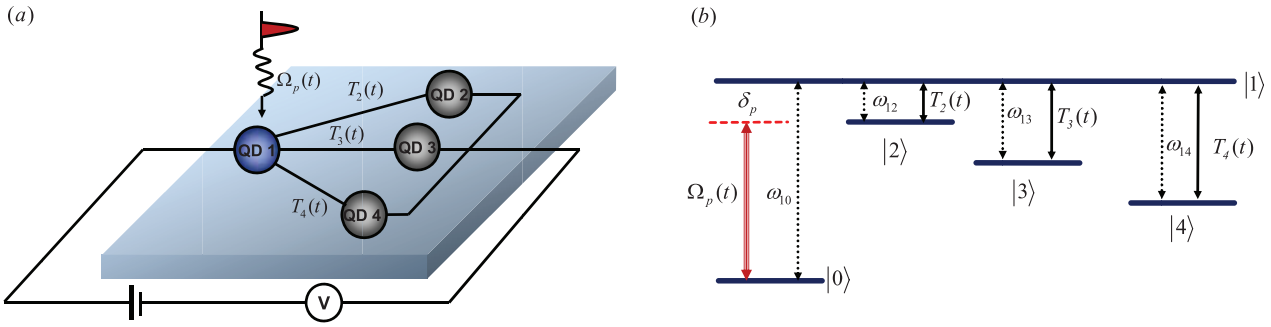

Figure 1. (a) The schematic of the setup of the QQDs. (b) The schematic of the level configuration of the QQDs.

molecules (QDMs). In QDMs, the tunneling between the QDs can be used to induce quantum coherence. Vertical and lateral types of QDMs can be experimentally fabricated by the self-assembled dot growth method, and the number of QDs per molecule can be controlled by the growth conditions [23–31]. Additionally, theoretical and experimental studies into generating and employing coherence in QDMs [32–49] have been reported.

The STIRAP technique has proven to be a robust and efficient way for complete or selective coherent population transfer between two discrete states [7–10]. Via this process, coherent control of the atomic system to a particular state [50, 51] or coherent creation and manipulation of superposition states [52–55] can be obtained. Although coherent population transfer in double quantum dots (DQDs) has also been reported [56, 57], there is no investigation into transfer and manipulation of coherence in QDMs. Therefore, in this paper, we report a method to transfer and manipulate coherence among the ground state and indirect exciton states of quadruple quantum dots (QQDs) and multiple quantum dots (MQDs) via groups of pump and tunneling pulses. By varying the amplitudes and sequences of pump and tunneling pulses, we can obtain a complete transfer of coherence or an arbitrary distribution of coherence among multiple states. In the whole process, the population can transfer from the initial ground state to the indirect exciton states without populating the direct exciton state, and thus no spontaneous emission takes place. Furthermore, in such a system, the tunneling pulses are controlled by the external voltage, so unlike the process of STIRAP, no additional laser pulses are needed.

2. Quadruple quantum dots

We consider lateral QQDs containing four self-assembled InAs QDs, and the schematic of the setup of QQDs is shown in figure 1(a). Experimentally, such semiconductor structure can be fabricated by molecular-beam epitaxy, and the number of QDs per molecule can be controlled by the InAs growth conditions. In QQDs, each QD can have different optical transition energies and can be optically addressable with a resonant laser frequency. Additionally, by adjusting the voltage bias, the electrons in QQDs can coherently tunnel between the four dots. When the gate voltage is not applied, the conduction-band electron energy levels are out of resonance; therefore, the electron tunneling between the neighbor QDs is quite weak. On the contrary, when the gate voltage is applied, the conduction-band electron energy levels are resonant; therefore, the electron tunneling between the neighbor QDs becomes very strong. The hole tunneling is neglected due to the off-resonance of the valence-band energy levels in the latter.

Under the resonant coupling of a pumped laser field with QD1, an electron is excited in QD1. Then, with the tunneling, the electron can be transferred to other QDs. Thus, the QQD structure can be treated as a five-level system (figure 1(b)): the ground state $|0\rangle$, where there are no excitations in any QDs; the direct exciton state $|1\rangle$, where the electron and hole are both in QD1; the indirect exciton states $|n\rangle$ $(n = 2, 3, 4)$, where the hole remains in the first dot and the electron is in nth dot.

In the rotating-wave approximation, the expression of $H(t)$ under the coupling of the pump and tunneling pulses can be written as

$$H(t) = \hbar \begin{pmatrix} 0 & -\Omega_{\rm p}(t) & 0 & 0 & 0 \\ -\Omega_{\rm p}(t) & \delta_{\rm p} & -T_2(t) & -T_3(t) & -T_4(t) \\ 0 & -T_2(t) & \delta_{\rm p}-\omega_{12} & 0 & 0 \\ 0 & -T_3(t) & 0 & \delta_{\rm p}-\omega_{13} & 0 \\ 0 & -T_4(t) & 0 & 0 & \delta_{\rm p}-\omega_{14} \end{pmatrix}. \quad (1)$$

Here, $\Omega_p(t)$ is the Rabi frequency of the pump pulse, and $T_i(t)$ $(i = 2, 3, 4)$ are the tunneling pulses, which can be controlled by varying the bias voltage. In the following calculations, $\Omega_{\rm p}$ and T_i $(i = 2, 3, 4)$ denote the peak value of the pump and tunneling pulses, and all the pulses have the same pulse duration T. The energy splitting of the direct exciton state $|1\rangle$ and ground state $|0\rangle$ is ω_{10}, and the energy splitting of the direct exciton state $|1\rangle$ and indirect exciton states $|i\rangle$ $(i = 2, 3, 4)$ is $\omega_{1i} = \omega_1 - \omega_i$ $(i = 2, 3, 4)$, with $\hbar\omega_i$ being the energy of the state $|i\rangle$. $\delta_{\rm p} = \omega_{10} - \omega_{\rm p}$ denotes the pump detuning ($\omega_{\rm p}$ is the frequency of the pump pulse). Additionally, in QQDs the energy splitting ω_{1i} depends on the effective confinement potential and is much smaller than ω_{10}. For simplicity, $\delta_{\rm p}$ and ω_{1i} are time-independent.

At any time t, the state vector can be written as

$$|\Psi(t)\rangle = a_0(t)|0\rangle + a_1(t)|1\rangle + a_2(t)|2\rangle + a_3(t)|3\rangle + a_4(t)|4\rangle. \tag{2}$$

The time evolution of the probability amplitude $A(t) = [a_0(t), a_1(t), a_2(t), a_3(t), a_4(t)]^{\mathrm{T}}$ can be described by the Schrödinger equation

$$\frac{\mathrm{d}}{\mathrm{d}t}A(t) = -\frac{\mathrm{i}}{\hbar}H(t)A(t) - \Lambda A(t), \tag{3}$$

where Λ is dissipative process, which contains two elements: spontaneous decay process and pure dephasing. Substituting equations (1) and (2) into equation (3), we can obtain the following dynamical equations for atomic probability amplitudes in the interaction picture

$$\mathrm{i}\dot{a}_0 = -\Omega_{\mathrm{p}}a_1, \tag{4a}$$

$$\mathrm{i}\dot{a}_1 = -\Omega_{\mathrm{p}}a_0 - T_2a_2 - T_3a_3 - T_4a_4 + (\delta_{\mathrm{p}} - \mathrm{i}\gamma_1)a_1, \tag{4b}$$

$$\mathrm{i}\dot{a}_2 = -T_2a_1 + (\delta_{\mathrm{p}} - \omega_{12} - \mathrm{i}\gamma_2)a_2, \tag{4c}$$

$$\mathrm{i}\dot{a}_3 = -T_3a_1 + (\delta_{\mathrm{p}} - \omega_{13} - \mathrm{i}\gamma_3)a_3, \tag{4d}$$

$$\mathrm{i}\dot{a}_4 = -T_4a_1 + (\delta_{\mathrm{p}} - \omega_{14} - \mathrm{i}\gamma_4)a_4. \tag{4e}$$

Here, $\gamma_i = \frac{1}{2}\Gamma_{i0} + \gamma_{i0}^{\mathrm{d}}$ $(i = 1 - 4)$ is the typical effective decay rate, with Γ_{i0} being the radiative decay rate of populations from $|i\rangle \to |0\rangle$ and γ_{i0}^{d} being the pure dephasing rates.

In the following, we will investigate the transfer and manipulation of coherence among ground state and indirect exciton states of QQDs via multiple tunneling; therefore, the time evolutions of population of each state and the coherence dynamics between the ground state and indirect exciton states are necessary. The density matrix element is

$$|\rho_{ij}| = |a_i^* a_j|. \tag{5}$$

If $i = j$, $|\rho_{ij}|$ represents the time evolutions of population P_i $(i = 0 - 4)$, while if $i \neq j$, $|\rho_{ij}|$ represents the coherence dynamics.

In our calculations, the realistic values of QDM parameters are $\hbar T_{2,3,4} \sim 1 - 10\,\mathrm{meV}$, $\hbar\gamma_1 \sim 0.002 - 0.01\,\mathrm{meV}$ and $\gamma_2 = \gamma_3 = \gamma_4 = 10^{-3}\gamma_1$ [42]. For simplicity, the pump-pulse detuning and the energy splitting are supposed to be zero. With these parameters the adiabatic condition can be fully satisfied. Moreover, the initial population is assumed to be in state $|0\rangle$, that is, $a_0(-\infty) = 1$, $a_n(-\infty) = 0$ $(n = 1, 2, 3, 4)$.

Our first aim is to transfer coherence among the ground state and the indirect exciton states, and we show the corresponding results in figure 2. The sequence of pump and tunneling pulses can be separated by three steps (Step-I, Step-II and Step-III: see figure 2(a)).

First, in the left column, Step-I prepares the coherence between state $|0\rangle$ and state $|2\rangle$ by using the fractional-STIRAP (F-STIRAP) among states $|0\rangle$, $|1\rangle$ and $|2\rangle$ [53]. With the pump pulse $\Omega_{\mathrm{p}}(t)$ and tunneling pulse $T_2(t)$ (left column of figure 2(a)), the system-state vector goes to

$$|\Psi_{-\mathrm{I}}\rangle = \cos\theta|0\rangle - \sin\theta|2\rangle. \tag{6}$$

Here, $\tan\theta = \Omega_{\mathrm{p}}(t)/T_2(t)$, with θ being the first mixing angle. In this step, according to equation (5), the population of the ground state $|0\rangle$ and indirect exciton state $|2\rangle$ are $|\cos\theta|^2$ and $|\sin\theta|^2$, respectively, while the population in the direct exciton state $|1\rangle$ and indirect exciton states $|3\rangle$ and $|4\rangle$ are zero, for $|\Psi_{-\mathrm{I}}\rangle$ has no component of these three states. Moreover, only the coherence $|\rho_{02}|$ is not zero, which is $|\cos\theta\,\sin\theta|$. With the same value of $\Omega_{\mathrm{p}-\mathrm{I}}$ and $T_{2-\mathrm{I}}$, at the end of Step-I, $|\Psi_{-\mathrm{I}}\rangle = (|0\rangle - |2\rangle)/\sqrt{2}$; thus $P_{0-\mathrm{I}} = P_{2-\mathrm{I}} = 1/2$ and $|\rho_{02-\mathrm{I}}| = 1/2$. As in the left column of figures 2(b) and (c) reveals, half of the population is transferred from state $|0\rangle$ to state $|2\rangle$, and coherence $|\rho_{02}|$ rises from zero to 1/2.

Second, in the middle column, we transfer the coherence from ρ_{02} to ρ_{03} in Step-II by using the STIRAP among states $|1\rangle, |2\rangle$ and $|3\rangle$. The pulse sequences of tunneling $T_2(t)$ and $T_3(t)$ are shown in the middle column of figure 2(a). During this process, the probability amplitude of $|0\rangle$ is unchanged, while the probability amplitude of $|2\rangle$ is changed to the superposition states of $|2\rangle$ and $|3\rangle$. Thus, the system-state vector goes to

$$|\Psi_{-\mathrm{II}}\rangle = [|0\rangle - (\cos\phi|2\rangle - \sin\phi|3\rangle)]/\sqrt{2}. \tag{7}$$

Here, $\tan\phi = T_2(t)/T_3(t)$ with ϕ being the second mixing angle. In this step, the population $P_{0-\mathrm{II}} = 1/2$, $P_{2-\mathrm{II}} = |\cos\phi|^2/2$ and $P_{3-\mathrm{II}} = |\sin\phi|^2/2$, while $P_{1-\mathrm{II}} = P_{4-\mathrm{II}} = 0$. And the coherence $|\rho_{02-\mathrm{II}}| = |\cos\phi|/\sqrt{2}$, $|\rho_{03-\mathrm{II}}| = |\sin\phi|/\sqrt{2}$ and $|\rho_{23-\mathrm{II}}| = |\cos\theta\,\sin\theta|$, while the other coherence remains zero. At the end of Step-II, $|\Psi_{-\mathrm{II}}\rangle$ goes to $(|0\rangle + |3\rangle)/\sqrt{2}$; thus $P_{0-\mathrm{II}} = P_{3-\mathrm{II}} = 1/2$ and $|\rho_{03-\mathrm{II}}| = 1/2$. As can be seen in the middle column of figures 2(b) and (c), the population in state $|2\rangle$ is completely transferred to state $|3\rangle$, and the population in state $|0\rangle$ is unchanged. Meanwhile, the coherence between state $|0\rangle$ and state $|2\rangle$ is fully transferred to that between state $|0\rangle$ and state $|3\rangle$.

Third, in the right column, we transfer the coherence from ρ_{03} to ρ_{04} in Step-III by using the STIRAP among states $|1\rangle$, $|3\rangle$ and $|4\rangle$. The pulse sequences of tunneling $T_3(t)$ and $T_4(t)$ are shown in the right column of figure 2(a). During this process, the probability amplitude of $|0\rangle$ is unchanged, while the probability amplitude of $|3\rangle$ is changed to the superposition states of $|3\rangle$ and $|4\rangle$. In this case, the system-state vector goes to

$$|\Psi_{-\mathrm{III}}\rangle = [|0\rangle + (\cos\varphi|3\rangle - \sin\varphi|4\rangle)]/\sqrt{2}. \tag{8}$$

Here, $\tan\varphi = T_3(t)/T_4(t)$ with φ being the third mixing angle. In this step, the population $P_{0-\mathrm{III}} = 1/2$, $P_{3-\mathrm{III}} = |\cos\varphi|^2/2$ and $P_{4-\mathrm{III}} = |\sin\varphi|^2/2$, while $P_{1-\mathrm{III}} = P_{2-\mathrm{III}} = 0$. The coherence $|\rho_{03-\mathrm{III}}| = |\cos\phi|/\sqrt{2}$, $|\rho_{04-\mathrm{III}}| = |\sin\phi|/\sqrt{2}$ and

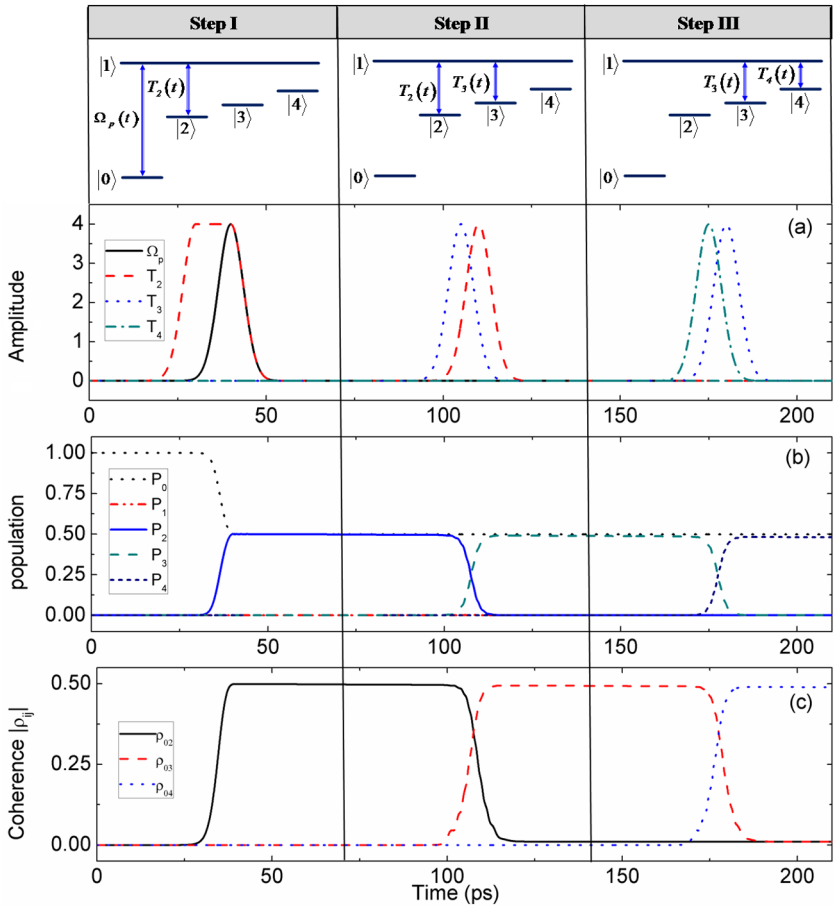

Figure 2. (a) The pump and the tunneling pulses, (b) the time evolutions of population P_i ($i = 0 - 4$), (c) the coherence dynamics $|\rho_{ij}|$. The peak value of $\hbar\Omega_p$, $\hbar T_2$, $\hbar T_3$ and $\hbar T_4$ in three steps are all 4 meV, $T = 5$ ps, $\hbar\gamma_1 = 0.01$ meV and $\gamma_2 = \gamma_3 = \gamma_4 = 10^{-3}\gamma_1$.

$|\rho_{34-\mathrm{III}}| = |\cos\theta \sin\theta|$, while other coherence becomes zero. At the end of Step-III, $|\Psi_{-\mathrm{III}}\rangle = (|0\rangle - |4\rangle)/\sqrt{2}$; thus $P_{0-\mathrm{III}} = P_{4-\mathrm{III}} = 1/2$ and $|\rho_{04-\mathrm{III}}| = 1/2$. So at last, the population in state $|3\rangle$ is completely transferred to state $|4\rangle$, and the population in state $|0\rangle$ is kept unchanged (right column of figure 2(b)). At the same time, the coherence between state $|0\rangle$ and state $|3\rangle$ is fully transferred to that between state $|0\rangle$ and state $|4\rangle$ (the right column of figure 2(c)).

So during these three steps, the population in the ground state can be transferred to the indirect exciton states, without populating the direct exciton states. Most important, the coherence transfer among the ground state and the indirect exciton states can be obtained.

In the following, we will try to obtain the coherence transfer by using the pump and tunneling pulses with the same amplitudes, but the different sequences, and we show the corresponding results in figure 3. The whole process can also be separated into three steps and the pump pulse and tunneling pulses are shown in figure 3(a).

The first step is the same as that in figure 2, therefore, at the end of Step-I, $|\Psi_{-\mathrm{I}}\rangle = (|0\rangle - |2\rangle)/\sqrt{2}$, and half of the population is transferred from state $|0\rangle$ to state $|2\rangle$, and coherence $|\rho_{02}|$ rises from zero to 1/2 (left column of figures 3(b) and (c)).

Second, in Step-II, we use STIRAP among states $|0\rangle$, $|1\rangle$ and $|3\rangle$ by applying the pump and tunneling pulses $\Omega_p(t)$ and $T_3(t)$ (middle column of figure 3(a)). During this process, the probability amplitude of $|2\rangle$ is unchanged, while the probability amplitude of $|0\rangle$ is changed to the superposition states of $|0\rangle$ and $|3\rangle$. In this case, the system-state vector goes to

$$|\Psi_{-\mathrm{II}}\rangle = [(\cos\phi|0\rangle - \sin\phi|3\rangle) - |2\rangle]/\sqrt{2}. \qquad (9)$$

Here, $\tan\phi = \Omega_p(t)/T_3(t)$ with ϕ being the second mixing angle. At the end of Step-II, $|\Psi_{-\mathrm{II}}\rangle$ goes to $(-|2\rangle - |3\rangle)/\sqrt{2}$. As can be seen in the middle column of figure 3(b), the population in state $|0\rangle$ is completely transferred to state $|3\rangle$, and the population in state $|2\rangle$ is unchanged. However, the middle column of figure 3(c) reveals that the coherence $|\rho_{02-\mathrm{II}}|$ and $|\rho_{03-\mathrm{II}}|$ both decreases to zero at the end of Step-II.

Third, in Step-III, we use STIRAP among states $|0\rangle$, $|1\rangle$ and $|4\rangle$ by applying the pump and tunneling pulses $\Omega_p(t)$ and $T_4(t)$ (right column of figure 3(a)). Since the initial system-state vector is $(-|2\rangle - |3\rangle)/\sqrt{2}$ and all of the population is in states $|2\rangle$ and $|3\rangle$, the state vector remains the same and no population is transferred. As can be seen in the right column

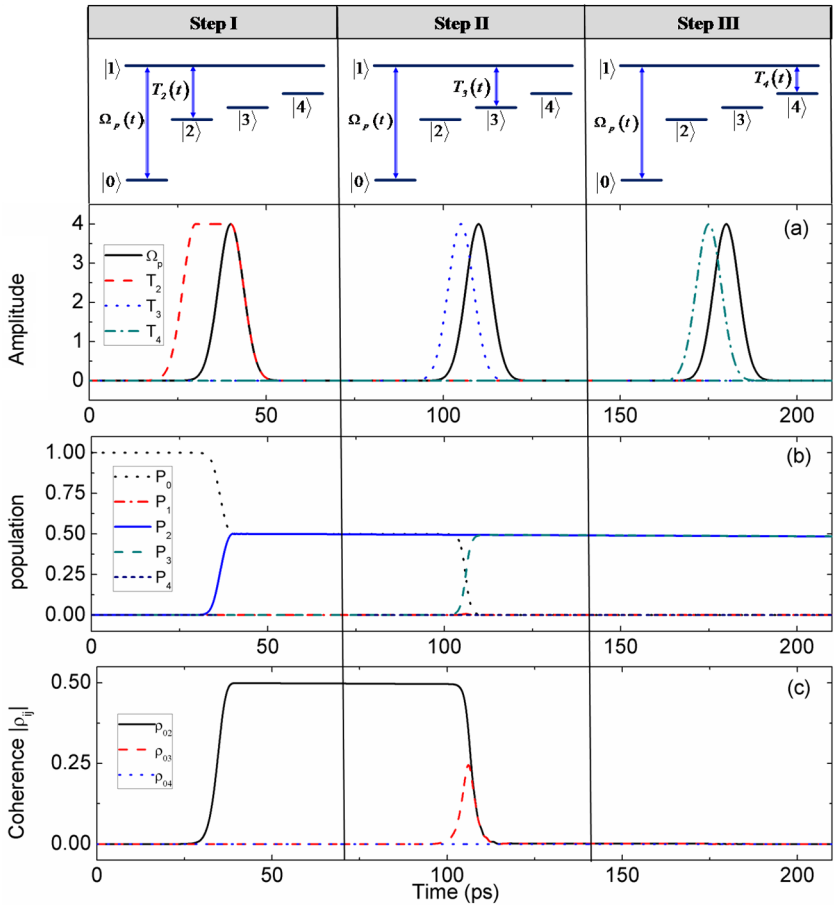

Figure 3. (a) The pump and the tunneling pulses, (b) the time evolutions of population P_i ($i = 0 - 4$), (c) the coherence dynamics $|\rho_{ij}|$. All the parameters are the same as those used in figure 2.

of figures 3(b) and (c), during this last step, the population of each state is unchanged; therefore, all the coherence $|\rho_{02}|$, $|\rho_{03}|$ and $|\rho_{04}|$ remains zero.

Comparing the results in figures 2 and 3, it can be concluded that the different pulses sequences may result in the different population and coherence distribution, although the amplitudes of the pump and tunneling pulses are the same.

Our next aim is to control the coherence distribution in QQDs. In figure 4, we use the pulses with the same pulses sequences as in figure 2, but with different pulse amplitudes. The whole process can be separated by three F-STIRAP steps, and as in the above analysis, the system-state vector in each step can be easily obtained. These are

$$|\Psi_{-\mathrm{I}}\rangle = \cos\theta|0\rangle - \sin\theta|2\rangle, \quad (10a)$$

$$|\Psi_{-\mathrm{II}}\rangle = \cos\theta|0\rangle - \sin\theta(\cos\phi|2\rangle - \sin\phi|3\rangle), \quad (10b)$$

$$|\Psi_{-\mathrm{III}}\rangle = \cos\theta|0\rangle - \sin\theta\Big[\cos\phi|2\rangle - \sin\phi\big(\cos\varphi|3\rangle - \sin\varphi|4\rangle\big)\Big], \quad (10c)$$

where $\tan\theta = \Omega_{\mathrm{p}}(t)/T_2(t)$, $\tan\phi = T_2(t)/T_3(t)$, and $\tan\varphi = T_3(t)/T_4(t)$. Correspondingly, the amplitudes of population and coherence in each step can be obtained by equation (5) and are relative to the three mixing angles θ, ϕ and φ.

First, in the left column, Step-I prepares the coherence between state $|0\rangle$ and state $|2\rangle$ by using the first F-STIRAP among states $|0\rangle$, $|1\rangle$ and $|2\rangle$. The ratio of the peak value $\Omega_{\mathrm{p-I}}$ and $T_{2-\mathrm{I}}$ is $\sqrt{3}$ (left column of figure 4(a)). As can be seen from the left column of figures 4(b) and (c), at the end of the step, the population in state $|0\rangle$ decreases from 1 to 1/4, while the population in state $|2\rangle$ increases from 0 to 3/4. Meanwhile, the coherence $|\rho_{02-\mathrm{I}}|$ rises from zero to $\sqrt{3}/4$.

Second, in the middle column, we distribute the obtained coherence to ρ_{02}, ρ_{03} and ρ_{23} in Step-II by using the second F-STIRAP among states $|1\rangle$, $|2\rangle$ and $|3\rangle$. The ratio of the peak value $T_{2-\mathrm{II}}$ and $T_{3-\mathrm{II}}$ is $\sqrt{2}$ (middle column of figure 4(a)). As can be seen in the middle column of figure 4(b), some of the population in state $|2\rangle$ is transferred to state $|3\rangle$ during Step-II, with the final value of them being $P_{2-\mathrm{II}} = 1/4$ and $P_{3-\mathrm{II}} = 1/2$, respectively. The population in state $|0\rangle$ is unchanged. Meanwhile, the coherence between state $|0\rangle$ and state $|2\rangle$ is distributed among states $|0\rangle$, $|2\rangle$ and $|3\rangle$, with the final value of them being $|\rho_{02-\mathrm{II}}| = 1/4$ and $|\rho_{03-\mathrm{II}}| = |\rho_{23-\mathrm{II}}| = \sqrt{2}/4$ (middle column of figure 4(c)).

Third, in the right column, we distribute the coherence among the desired states in Step-III by using the third F-STIRAP among states $|1\rangle$, $|3\rangle$ and $|4\rangle$. The ratio of the

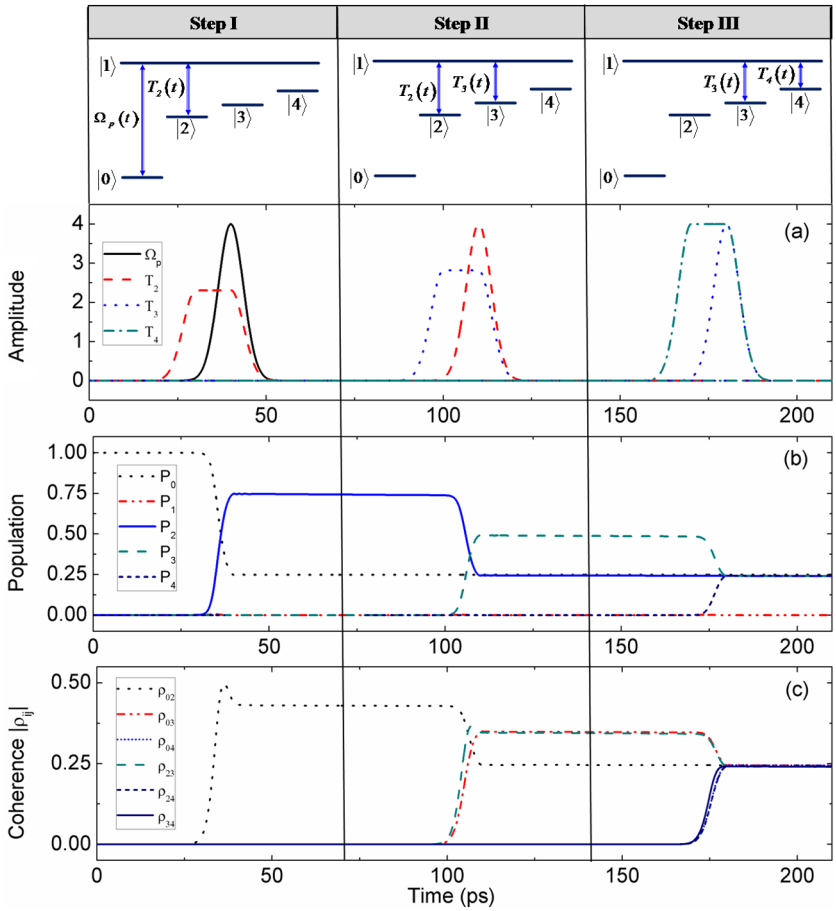

Figure 4. (a) The pump and the tunneling pulses, (b) the time evolutions of population P_i ($i = 0 - 4$), (c) the coherence dynamics $|\rho_{ij}|$. $\hbar\Omega_{\mathrm{p-I}} = 4$ meV, $\hbar T_{2-\mathrm{I}}=(4/\sqrt{3})$meV, $\hbar T_{2-\mathrm{II}} = 4$ meV, $\hbar T_{3-\mathrm{II}} = (4/\sqrt{2})$meV, $\hbar T_{3-\mathrm{III}} = 4$ meV and $\hbar T_{4-\mathrm{III}} = 4$ meV. Other parameters are the same as those used in figure 2.

peak values $T_{3-\mathrm{III}}$ and $T_{4-\mathrm{III}}$ are the same (right column of figure 4(a)). In this last step, half of the population in state $|3\rangle$ is transferred to state $|4\rangle$; thus the population is equally distributed among the four states $|0\rangle$, $|2\rangle$, $|3\rangle$ and $|4\rangle$, and state $|1\rangle$ is empty during the whole process (the right column of figure 4(b)). Furthermore, as the right column of figure 4(c) revealed that the coherence of ρ_{03} and ρ_{23} transferred to that of ρ_{04}, ρ_{24} and ρ_{34}, the coherence is equally distributed to the coherence among the ground state $|0\rangle$ and the three indirect exciton states $|2\rangle$, $|3\rangle$ and $|4\rangle$, with the entire value being $|\rho_{ij-\mathrm{III}}| = 1/4$ ($i,j = 0, 2, 3, 4$; $i < j$). So by using three F-STIRAP processes and choosing the suitable value of the amplitude of the pump and the tunneling pulses, we successfully distribute the coherence among the desired states, and the results coincide with the coherence amplitude equations.

Then, we will show that the coherence distribution can also be achieved by other pulse sequences. In figure 5, we use the pulses with the same pulses sequences as that of figure 3, but with the different pulse amplitudes. The whole process can also be separated by three F-STIRAP steps; thus the system-state vectors in each step are

$$|\Psi_{-\mathrm{I}}\rangle = \cos\theta|0\rangle - \sin\theta|2\rangle, \quad (11a)$$

$$|\Psi_{-\mathrm{II}}\rangle = \cos\theta(\cos\phi|0\rangle - \sin\phi|3\rangle) - \sin\theta|2\rangle. \quad (11b)$$

$$|\Psi_{-\mathrm{III}}\rangle = \cos\theta\Big[\cos\phi\big(\cos\varphi|0\rangle - \sin\varphi|4\rangle\big) - \sin\phi|3\rangle\Big] - \sin\theta|2\rangle, \quad (11c)$$

where $\tan\theta = \Omega_{\mathrm{p}}(t)/T_2(t)$, $\tan\phi = \Omega_{\mathrm{p}}(t)/T_3(t)$, and $\tan\varphi = \Omega_{\mathrm{p}}(t)/T_4(t)$. Correspondingly, the amplitudes of population and coherence in each step can be obtained by equation (5) and are relative to the three mixing angles θ, ϕ and φ.

First, in Step-I, the ratio of the peak value $\Omega_{\mathrm{p-I}}$ and $T_{2-\mathrm{I}}$ used in the first F-STIRAP process is $1/\sqrt{3}$, as shown in the left column of figure 5(a). Thus, the population in state $|0\rangle$ decreases from 1 to 3/4, while the population in state $|2\rangle$ increases from zero to 1/4. Meanwhile, the coherence $|\rho_{02-\mathrm{I}}|$ rises from zero to $\sqrt{3}/4$ at the end of the step (left column of figures 5(b) and (c)).

Second, in Step-II, we distribute the obtained coherence to ρ_{02}, ρ_{03} and ρ_{23}, and the ratio of the peak value $\Omega_{p-\mathrm{II}}$ and $T_{3-\mathrm{II}}$ used in the second F-STIRAP process is $1/\sqrt{2}$ (middle column of figure 5(a)). As shown in the middle column of figures 5(b) and (c), some of the population in state $|0\rangle$ is transferred to state $|3\rangle$ with the value of them being $P_{0-\mathrm{II}} = 1/2$ and $P_{3-\mathrm{II}} = 1/4$,

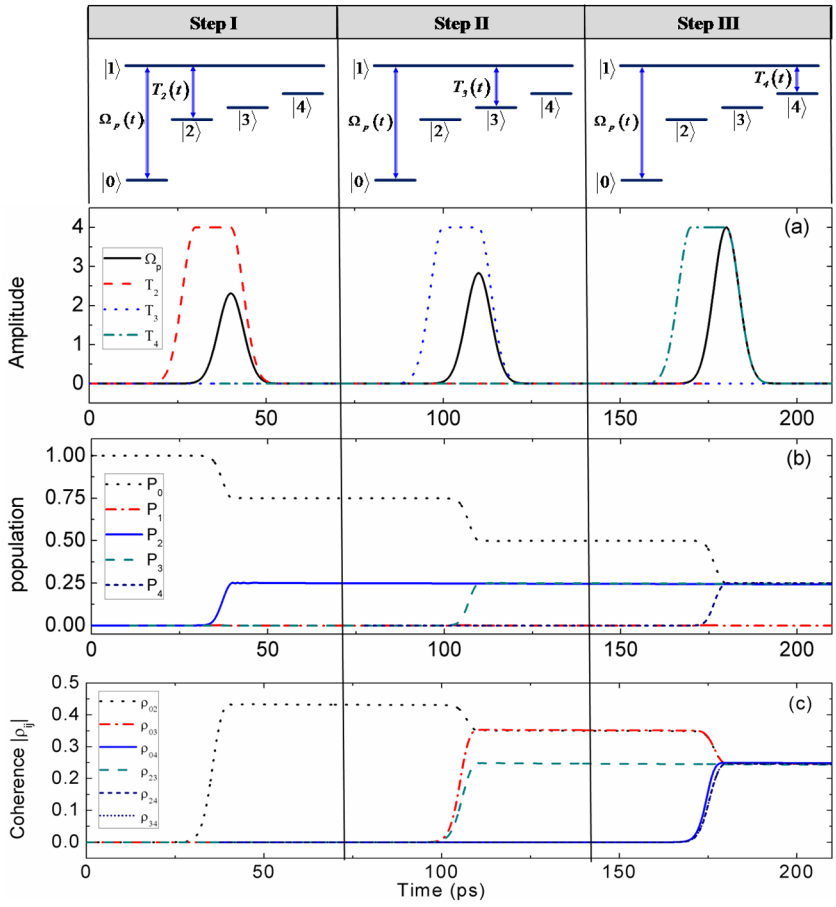

Figure 5. (a) The pump and the tunneling pulses, (b) the time evolutions of population P_i $(i = 0 - 4)$, (c) the coherence dynamics $|\rho_{ij}|$. $\hbar\Omega_{p-\mathrm{I}} = (4/\sqrt{3})$meV, $\hbar T_{2-\mathrm{I}} = 4$meV, $\hbar\Omega_{p-\mathrm{II}} = (4/\sqrt{2})$meV, $\hbar T_{3-\mathrm{II}} = 4$ meV, $\hbar\Omega_{p-\mathrm{III}} = 4$ meV and $\hbar T_{4-\mathrm{III}} = 4$ meV. Other parameters are the same as those used in figure 2.

respectively. Meanwhile, the coherence value among states $|0\rangle, |2\rangle$ and $|3\rangle$ is $|\rho_{02-\mathrm{II}}| = |\rho_{03-\mathrm{II}}| = \sqrt{2}/4$ and $|\rho_{23-\mathrm{II}}| = 1/4$.

Third, in Step-III, we distribute the coherence among the desired states by using the third F-STIRAP process. The ratio of the peak value $\Omega_{\mathrm{p-III}}$ and $T_{4-\mathrm{III}}$ are 1 (right column of figure 5(a)). In this situation, some of the population in state $|0\rangle$ is transferred to state $|4\rangle$, and finally all the ground state $|0\rangle$ and the indirect exciton states $|2\rangle, |3\rangle$ and $|4\rangle$ have an equal population (the right column of figure 5(b)). Also, as the right column of figure 5(c) reveals, the coherence is distributed equally to $|\rho_{ij-\mathrm{III}}|$ $(i, j = 0, 2, 3, 4;\ i < j)$, with the value being 1/4.

Comparing the results in figures 4 and 5, it can be concluded that by applying suitable amplitudes of the pump and the tunneling pulses, even when the pulse sequences are different, the equal distribution of population and coherence among the ground state and the indirect exciton states is possible.

3. Multiple quantum dots

To obtain a general case, the MQDs are also analyzed. The number of QDs is N and it can be controlled by the growth conditions. In MQDs each QD can have different optical transition energies and can be optically addressable with a resonant laser frequency. By adjusting the voltage bias, the electrons in MQDs can coherently tunnel between the dots, and the hole tunneling is neglected. Under the resonant coupling of a pumped laser field with QD1, an electron is excited in the latter. Then, with the tunneling, the electron can be transferred to other QDs. Thus, the MQDs can be treated as an $N+1$ level system (figure 6(b): the ground state $|0\rangle$, where there are no excitations in any QDs; the direct exciton state $|1\rangle$, where the electron and hole are both in QD1; the indirect exciton states $|n\rangle$ $(n = 2, 3, ..., N)$, where the hole remains in the first dot and the electron is in the n-th dot.

The expression of $H(t)$ in the rotating-wave approximation can be written as

$$H(t) = \hbar \begin{pmatrix} 0 & -\Omega_{\mathrm{p}}(t) & 0 & \ldots & 0 \\ -\Omega_{\mathrm{p}}(t) & \delta_{\mathrm{p}} & -T_2(t) & \ldots & -T_N(t) \\ 0 & -T_2(t) & \delta_{\mathrm{p}} - \omega_{12} & \ldots & 0 \\ \vdots & \vdots & \vdots & \vdots & \vdots \\ 0 & -T_N(t) & 0 & \ldots & \delta_{\mathrm{p}} - \omega_{1N} \end{pmatrix}. \quad (12)$$

Here, $\Omega_{\mathrm{p}}(t)$ is the Rabi frequency of the pump pulse, $T_n(t)$ $(n = 2, 3, ..., N)$ are the tunneling pulses, which can

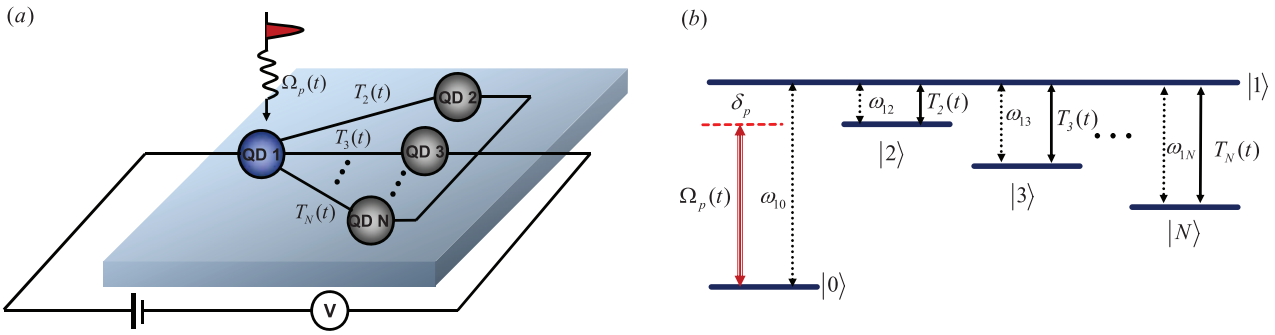

Figure 6. (a) The schematic of the setup of the MQDs. The pump pulse transmits QD 1. (b) The schematic of the level configuration of the MQDs.

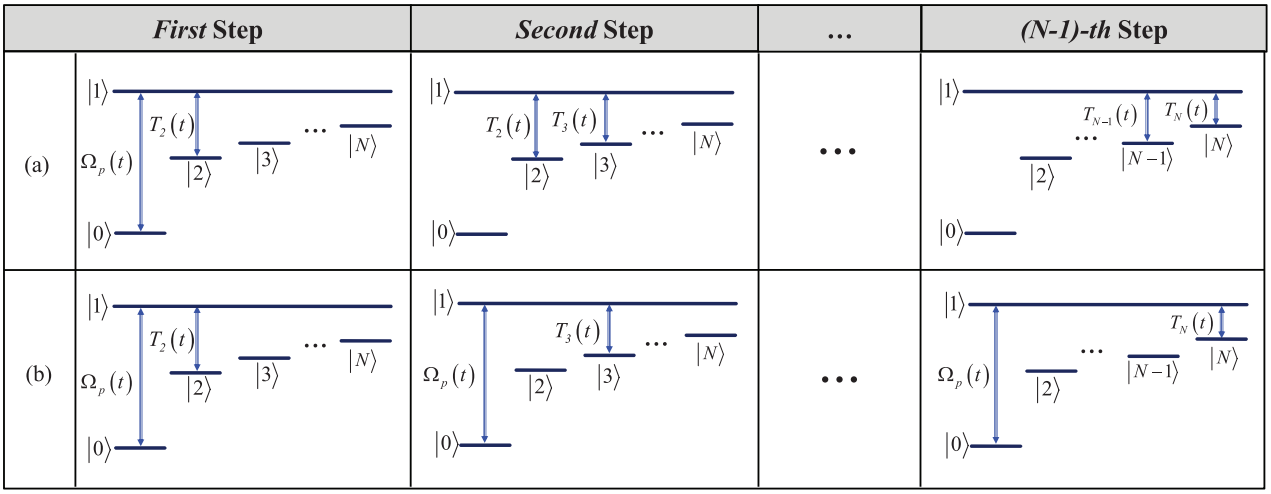

Figure 7. The pump and the tunneling pulses. (a) The first case; (b) the second case.

be controlled by varying the bias voltage. The energy splitting of the direct exciton state $|1\rangle$ and ground state $|0\rangle$ is ω_{10}, and the energy splitting of the direct exciton state $|1\rangle$ and indirect exciton states $|n\rangle$ $(n = 2, 3, ..., N)$ is $\omega_{1n} = \omega_1 - \omega_n$ $(n = 2, 3, ..., N)$, with $\hbar\omega_i$ being the energy of the state n $(n = 2, 3, ..., N)$. $\delta_p = \omega_{10} - \omega_p$ denotes the pump detuning (ω_p is the frequency of the pump pulse). At any time t, the state vector can be written as

$$|\Psi(t)\rangle = \sum_{n=0}^{N} a_n(t)|n\rangle. \tag{13}$$

Additionally, the time evolution of the probability amplitude is $A(t) = [a_0(t), a_1(t), ..., a_N(t)]^T$. From equation (3), the dynamical equations for atomic probability amplitudes in the interaction picture are

$$i\dot{a}_0 = -\Omega_p a_1, \tag{14a}$$

$$i\dot{a}_1 = -\Omega_p a_0 - \sum_{n=2}^{N} T_n a_n + (\delta_p - i\gamma_1)a_1, \tag{14b}$$

$$i\dot{a}_n = -T_n a_1 + (\delta_p - \omega_{1n} - i\gamma_n)a_n, \ (n = 2, 3, ..., N) \tag{14c}$$

where $\gamma_n = \frac{1}{2}\Gamma_{n0} + \gamma_{n0}^{d}$ $(n = 1, 2, ..., N)$ is the typical effective decay rate, with Γ_{n0} being the radiative decay rate of populations from $|n\rangle \to |0\rangle$ and γ_{n0}^{d} being the pure dephasing rates. The initial population is assumed to be in state $|0\rangle$, which means $a_0(-\infty) = 1$, $a_n(-\infty) = 0$ $(n = 1, 2, ..., N)$.

The creation and transfer of coherence in MQDs can be obtained by applying several sequences of pump and tunneling pulses. Here, we use $N - 1$ F-STIRAP processes. The sequence of the pulses can have many possibilities, but here we just give two cases for example.

The first case is shown in figure 7(a), which is similar to figure 4(a). It can be seen that $\Omega_p(t)$ is only used in the first step, $T_N(t)$ is only used in the last step, and the other tunnelings $T_n(t)$ $(n = 2, 3, ..., N - 1)$ are used in both $(n - 1)$th and nth steps. $T_2(t)$ precedes $\Omega_p(t)$ in the first step, and they are switched off simultaneously. And $T_{n+1}(t)$ precedes $T_n(t)$ in nth step, where $n = 2, 3, ..., N - 1$, and also two tunneling pulses are switched off simultaneously in each step. By using the first F-STIRAP process, the coherence between states $|0\rangle$ and $|2\rangle$ can be created. After other $N - 2$ F-STIRAP processes, the final state vector goes to

$$|\Psi\rangle = \cos\theta_1|0\rangle + \sum_{n=2}^{N-1}(-1)^{n-1}\sin\theta_1\sin\theta_2\cdots\sin\theta_{n-1}\cos\theta_n|n\rangle + (-1)^{N-1}\sin\theta_1\sin\theta_2\cdots\sin\theta_{N-2}\sin\theta_{N-1}|N\rangle, \tag{15}$$

where, $\theta_1 = \Omega_p(t)/T_2(t)$ and $\theta_n = T_n(t)/T_{n+1}(t)$ $(n = 2, 3, ..., N-1)$. Using equations (5) and (15), the coherence dynamics between the ground state and indirect exciton states can be calculated. Thus, by applying the suitable amplitudes of the pump and the tunneling pulses, the arbitrary distribution of coherence can be obtained. For example, equal distribution can be obtained by using the following peak value, $T_n = T_N/[N-(n-1)]^{0.5}$ $(n = 2, 3, ..., N-1)$ in the $(n-1)$-th step, $T_n = T_N$ $(n = 2, 3, ..., N)$ is the nth step, and $\Omega_p = T_N$.

Then we show the second case in figure 7(b), which is similar to figure 5(a). In this case, $\Omega_p(t)$ is used in all $N-1$ steps, and $T_n(t)$ $(n = 2, 3, ..., N)$ is used in $(n-1)$-*th* step. In each step $T_n(t)$ $(n = 2, 3, ..., N)$ precedes $\Omega_p(t)$, and they are switched off simultaneously. The coherence between states $|0\rangle$ and $|2\rangle$ can also be created by the first F-STIRAP process. Then, after other $N-2$ F-STIRAP processes, the final state vector goes to

$$|\Psi\rangle = \cos\theta_1 \cos\theta_2 \cdots \cos\theta_{N-1}|0\rangle - \sin\theta_1|2\rangle - \sum_{n=3}^{N} \cos\theta_1 \cdots \cos\theta_{n-2} \sin\theta_{n-1}|n\rangle, \quad (16)$$

where, $\theta_n = \Omega_p(t)/T_{n+1}(t)$ $(n = 1, 2, ..., N-1)$. Using equations (5) and (16), the coherence dynamics between the ground state and indirect exciton states can also be calculated. Therefore, the arbitrary distribution of coherence is possible by using suitable amplitudes of the pump and tunneling pulses. For instance, equal distribution can be obtained by using the following peak value, which is $\Omega_p = T_N/\sqrt{N-n}$ $(n = 1, 2, ..., N-1)$ in nth step, and all the tunneling pulses have the same value $T_n = T_N$ $(n = 2, 3, ..., N)$.

4. Conclusions

In this paper, we have theoretically demonstrated that it is possible to transfer and manipulate coherence among ground state and indirect exciton states in QQDs and MQDs via multiple tunneling pluses. We show that with the same amplitudes of the pump and the tunneling pulses, different pulse sequences may result in the different distribution of population and coherence, and on the other hand, with suitable amplitudes of the pump and tunneling pulses, different pulse sequences can still lead to the same equal distribution of population and coherence. Moreover, in the whole process the system-state vector has no component of the direct exciton state; thus no population occupies this state and no spontaneous emission occurs. Such semiconductor nanostructures have essential applications in quantum information processing based on the coherence effect, such as slow-light storage, quantum logical gates, and so on.

Acknowledgments

This work is supported by the financial support from the National Natural Science Foundation of China (Grant Nos. 11304308, 11204029, 11447232, 51501176, 61176046 and 61234004), the National Basic Research Program of China (Grant Nos. 2013CB933300), the International Science Technology Cooperation Program of China (Grant No. 2013DFR00730), and Jilin Provincial Natural Science Foundation (Grant Nos. 20140101203JC and 20160520095JH).

References

[1] Arimondo E and Orriols G 1976 *Lett. Nuovo Cimento Soc. Ital. Fis.* **17** 333
[2] Alzetta G, Gozzini A, Moi A and Orriols G 1976 *Nuovo Cimento Soc. Ital. Fis.* B **36** 5
[3] Gray H R, Whitley R M and Stroud J C R 1978 *Opt. Lett.* **3** 218
[4] Harris S E 1997 *Phys. Today* **50** 36
[5] Marangos J P 1998 *J. Mod. Opt.* **45** 471
[6] Fleischhauer M, Imamoglu A and Marangos J P 2005 *Rev. Mod. Phys.* **77** 633
[7] Bergmann K, Theuer H and Shore B W 1998 *Rev. Mod. Phys.* **70** 1003
[8] Vitanov N V, Fleischhauer M, Shore B W and Bergmann K 2001 *Adv. Atom. Mol. Opt. Phys.* **46** 55
[9] Kral P, Thanopulos I and Shapiro M 2007 *Rev. Mod. Phys.* **79** 53
[10] Bergmann K, Vitanov N V and Shore B W 2015 *J. Chem. Phys.* **142** 170901
[11] Yatsenko L P, Shore B W, Halfmann T, Bergmann K and Vardi A 1999 *Phys. Rev.* A **60** R4237
[12] Yatsenko L P, Vitanov N V, Shore B W, Rickes T and Bergmann K 2002 *Opt. Commun.* **204** 413
[13] Agarwal G S 1974 *Quantum Optics* (Berlin: Springer)
[14] Zhu S Y and Scully M O 1996 *Phys. Rev. Lett.* **76** 388
[15] Wu J H and Gao J Y 2002 *Phys. Rev.* A **65** 063807
[16] Wang C L, Kang Z H, Tian S C, Jiang Y and Gao J Y 2009 *Phys. Rev.* A **79** 043810
[17] Tian S C, Kang Z H, Wang C L, Wan R G, Kou J, Zhang H, Jiang Y, Cui H N and Gao J Y 2012 *Opt. Commun.* **285** 294
[18] Krauss T F 2008 *Nat. Photon.* **2** 448
[19] Kamada H, Gotoh H, Temmyo J, Takagahara T and Ando H 2001 *Phys. Rev. Lett.* **87** 246401
[20] Stievater T H, Li X, Steel D G, Gammon D, Katzer D S, Park D, Piermarocchi C and Sham L J 2001 *Phys. Rev. Lett.* **87** 133603
[21] Htoon H, Takagahara T, Kulik D, Baklenov O, Holmes A L and Shih C K 2002 *Phys. Rev. Lett.* **88** 087401
[22] Zrenner A, Beham E, Stufler S, Findeis F, Bichler M and Abstreiter G 2002 *Nature* **418** 612
[23] Xie Q, Madhukar A, Chen P and Kobayashi N P 1995 *Phys. Rev. Lett.* **75** 2542
[24] Hayne M, Provoost R, Zundel M K, Manz Y M, Eberl K and Moshchalkov V V 2000 *Phys. Rev.* B **62** 10324
[25] Bayer M, Hawrylak P, Hinzer K, Fafard S, Korkusinski M, Wasilewski Z R, Stern O and Forchel A 2001 *Science* **291** 451
[26] Songmuang R, Kiravittaya S and Schmidt O G 2003 *Appl. Phys. Lett.* **82** 2892
[27] Lee J H, Wang Z M, Strom N W, Mazur Y I and Salamo G J 2006 *Appl. Phys. Lett.* **89** 202101
[28] Beirne G J, Hermannstädter C, Wang L, Rastelli A, Schmidt O G and Michler P 2006 *Phys. Rev. Lett.* **96** 137401
[29] Popescu V, Bester G, Hanna M C, Norman A G and Zunger A 2008 *Phys. Rev.* B **78** 205321
[30] Wang L, Rastelli A, Kiravittaya S, Benyoucef M and Schmidt O G 2009 *Adv. Mater.* **21** 2601

[31] Chang-Yu H, Yun-Pil, S Marek K and Pawel H 2012 *Rep. Prog. Phys.* **75** 114501
[32] Paspalakis E 2003 *Phys. Rev.* B **67** 233306
[33] Villas-Bôas J M, Govorov A O and Ulloa S E 2004 *Phys. Rev.* B **69** 125342
[34] Unold T, Mueller K, Lienau C, Elsaesser T and Wieck A D 2005 *Phys. Rev. Lett.* **94** 137404
[35] Krenner H J, Sabathil M, Clark E C, Kress A, Schuh D, Bichler M, Abstreiter G and Finley J J 2005 *Phys. Rev. Lett.* **94** 057402
[36] Stinaff E A, Scheibner M, Bracker A S, Ponomarev I V, Korenev V L, Ware M E, Doty M F, Reinecke T L and Gammon D 2006 *Science* **311** 636
[37] Li J, Liu J and Yang X 2008 *Phys.* E **40** 2916
[38] Boyer de La Giroday A, Sköld N, Stevenson R M, Farrer I, Ritchie D A and Shields A J 2011 *Phys. Rev. Lett.* **106** 216802
[39] Kim D, Carter S G, Greilich A, Bracker A S and Gammon D 2011 *Nat. Phys.* **7** 223
[40] Müller K *et al* 2012 *Phys. Rev. Lett.* **108** 197402
[41] Weiss K M, Elzerman J M, Delley Y L, Miguel-Sanchez J and Imamoglu A 2012 *Phys. Rev. Lett.* **109** 107401
[42] Borges H S, Sanz L, Villas-Bôas J M, Diniz Neto O O and Alcalde A M 2012 *Phys. Rev.* B **85** 115425
[43] Sköld N, Boyer de La Giroday B, Bennett A J, Farrer I, Ritchie D A and Shields A J 2013 *Phys. Rev. Lett.* **110** 016804
[44] Tian S C, Wan R G, Tong C Z, Ning Y Q, Qin L and Liu Y 2014 *J. Opt. Soc. Am.* B **31** 1436
[45] Tian S C, Wan R G, Tong C Z and Ning Y Q 2014 *J. Opt. Soc. Am.* B **31** 2681
[46] Peng Y D, Yang A H, Li D H, Zhang H, Niu Y P and Gong S Q 2014 *Laser Phys. Lett.* **11** 065201
[47] Sahrai M, Mehmannavaz M R and Sattari H 2014 *Appl. Opt.* **53** 2375
[48] Tian S C, Wan R G, Tong C Z, Fu X H, Cao J S and Ning Y Q 2015 *Laser Phys. Lett.* **12** 125203
[49] Hamedi H R 2016 *J. Opt. Soc. Am.* B **33** 151
[50] Kuklinski J R, Gaubatz U, Hioe F T and Bergmann K 1989 *Phys. Rev.* A **40** 6741
[51] Coulston G W and Bergmann K 1992 *J. Chem. Phys.* **96** 3467
[52] Unanyan R, Fleischhauer M, Shore B W and Bergmann K 1998 *Opt. Commun.* **155** 144
[53] Vitanov N V, Suominen K A and Shore B W 1999 *J. Phys. B: At. Mol. Opt. Phys.* **32** 4535
[54] Niu Y P, Gong S Q, Li R X and Jin S Q 2004 *Phys. Rev.* A **70** 023805
[55] Wang L, Song X L, Li A J, Wang H H, Wei X G, Kang Z H, Jiang Y and Gao J Y 2008 *Opt. Lett.* **33** 2380
[56] Hohenester U, Troiani F, Molinari E, Panzarini G and Macchiavello C 2000 *Appl. Phys. Lett.* **77** 1864
[57] Fountoulakis A and Paspalakis E 2013 *J. Appl. Phys.* **113** 174301